ELSEVIER

Polymer 42 (2001) 8217–8223

polymer

www.elsevier.nl/locate/polymer

Morphology evolution of polycarbonate–polystyrene blends during compounding

C.Z. Chuai[a,b,*], K. Almdal[c], Ib Johannsen[b,c], J. Lyngaae-Jørgensen[b]

[a]*Department of Chemical Engineering, Tianjin Institute of Light Industry, 300222 Tianjin, The People's Republic of China*
[b]*Danish Polymer Centre, Building 423, Technical University of Denmark, DK-2800 Lyngby, Denmark*
[c]*Danish Polymer Centre, Risø National Laboratory, P.O. Box 49, DK-4000 Roskilde, Denmark*

Received 19 February 2001; received in revised form 11 April 2001; accepted 25 April 2001

Abstract

The morphology evolution of polycarbonate–polystyrene (PC/PS) blends during the compounding process in three blending methods of industrial relevance, namely melt blending, re-melt blending in a twin-screw extruder and tri-melt blending in an injection-moulding machine, was investigated using scanning electron microscopy (SEM) to examine nine blend compositions. Blends were prepared at compositions where phase inversion was expected to occur according to model predictions. The experimental results were compared to the values of the point of phase inversion calculated with the semi-empirical model. The results show that the formation of co-continuous morphology strongly depends on blend composition and melt blending method, whereas the model prediction for phase inversion deviates from the experimental values. Further, we found that the initial mechanism of morphology evolution involves the formation of blades or stratifications in the continuous phase. These blades or stratifications became unstable due to the effects of flow and interfacial forces. We also found that fibre formation in the dispersed phase was favoured by higher shear rate.

Keywords: Polymer blends; Blend morphology; Morphology evolution

1. Introduction

It is a long-standing interest of polymer researchers to understand the evolution of blend morphology when two incompatible homopolymers or copolymers are melt-blended in mixing equipment. Blending two polymers usually results in the formation of an immiscible heterogeneous two-phase system due to thermodynamic reasons [1]. When melt blending two immiscible homopolymers or random copolymers in mixing equipment, one encounters many types of blend morphology, such as co-continuous morphology and dispersed morphology. These morphologies can be seen as droplets, fibrils, strands, blades and lamellae. Since the morphology of polymer blends can affect many of physical and mechanical properties including impact strength, elongational properties, and permeability characteristics [2–7], it is of great importance to know how these complicated morphologies are formed in situ and can be controlled during compounding. In general, composition, viscosity ratio, molar mass, elasticity ratio, interfacial tension, shear rate/shear stress and mixing time play a critical role in the development of microstructure in immiscible polymer blends. Much research has already been undertaken to determine the relationship between morphology and these various factors [8–16]. However, work on morphology development during the mixing process has been reported by very few authors [17–21] and the evolution of morphologies during compounding process has not been fully explained. The nature of co-continuity, phase inversion and morphology evolution after melt blending or after re-melt blending in twin-screw extruders is quite limited. The effect of polymer/polymer blending in injection-moulding machines on morphology development is also unknown.

It is widely known that the polymer blending time in twin-screw extrusion or in injection-moulding is usually relatively short and this is very important for predicting and controlling the phase morphology of the blend in an industrial process.

In this study, we carried out a systematic experimental investigation on the evolution of blend morphology, using scanning electron microscopy (SEM), during melt blending of polycarbonate (PC) and polystyrene (PS) in a twin-screw

* Corresponding author. Present address: Danish Polymer Centre, Building 423, Technical University of Denmark, DK-2800 Lyngby, Denmark. Tel.: +45-4525-6808; fax: +45-4588-2161.
E-mail address: czc@polymers.dk (C.Z. Chuai).

0032-3861/01/$ - see front matter
PII: S0032-3861(01)00309-3

extruder and in an injection-moulding machine. For the investigation, nine compositions of PC/PS were selected and three blending operations, namely melt blending, re-melt blending in a twin-screw extruder and tri-melt blending in an injection-moulding machine, were applied.

2. Theoretical aspects

Dual-phase continuity is a special morphology in binary polymer blends where both phases maintain their whole continuity. This structure has significant impact on the physical and mechanical properties of polymer blends (e.g. transport properties) [8]. However, the complex microstructure can be difficult to characterise and describe. In general, the morphology of polymer blends is directly related to the viscoelastic properties of their individual components. The point of phase inversion, at which co-continuity is observed, can be related to the rheology of the pure materials through semi-empirical models. A semi-empirical expression has been proposed to predict the point of phase inversion based on the viscosity ratio [15,22]:

$$\frac{\eta_1}{\eta_2} = \frac{\phi_1}{\phi_2} \tag{1}$$

where η_i is the viscosity of polymer i at the shear rate of blending and ϕ_i is the volume fraction of polymer i. Substituting the torque ratio for the viscosity ratio, Avgeropoulos et al. [23] used a relationship between the torque ratio and the composition expressed as

$$\frac{T_1}{T_2} = \frac{\phi_1}{\phi_2} \tag{2}$$

where T_i is the torque of polymer i and ϕ_i is the volume fraction of polymer i. By using the torque ratio as the viscoelastic characteristic of the materials, Avgeropoulos et al. [23] included all forces, such as shearing and elongational forces, that act on the polymers during blending in an internal mixer.

3. Experimental

3.1. Materials

The PC used in this study was Makrolon CD 2005 from Bayer. The product is composed of amorphous pellets and its melt volume–flow rate is 60 cm^3/10 min (300°C, 1.2 kg load). The PS was Polystyrol 144 C from BASF. The product is also in the form of amorphous pellets and has a melt volume–flow rate of 28 cm^3/10 min (200°C, 5 kg load). The molar masses of the original components, as well as the blends, were measured by gel permeation chromatography before and after blending. No significant changes in molar mass were observed as a result of blending.

3.2. Sample preparation

The PC was dried for 14 h at 120°C in a vacuum oven to prevent hydrolysis of the PC during melt processing. The PC/PS blends were made manually by rolling the correct ratios of pellets in plastic bags. The weight fractions of PC were 0.94, 0.80, 0.60, 0.50, 0.40, 0.20 and 0.06, which combined with the pure polymer samples, constituted a series of nine combinations. Melt blending was executed in a Haake twin-screw extruder (Rheomex 252P) and in a Nissel vertical screw type injection-moulding machine (model THM 7). The extrudate from a rod die attached to the extruder was pulled through a water bath and immediately pelletized. The blended pellets were dried for 30 h at 80°C as before just prior to the re-melt extrusion by the same extruder and the third melt injection-moulding by a screw-type machine into specimens for measurement. The various heating zones for extrusion and injection-moulding were set in the range of 200–240°C for PS and gradually increased with the PC content to the range of 240–280°C for PC.

3.3. Morphological analysis

The morphology of all blends was examined using a JEOL JSM-5310 LV scanning electron microscope. The samples to be treated were prepared in two ways, either by cryofracturing in liquid nitrogen or by selectively dissolving away one component from the quenched samples to aid in identification. Cyclohexane was used as a selective solvent to dissolve the PS phase at 40°C in the PC/PS blends. The extraction and drying cycles were repeated several times until a constant weight of the remaining polymeric block was obtained. All sample surfaces were coated with 25 nm of a gold layer. For the best representation, scanning of the whole samples was done before the micrographs were taken.

3.4. Torque measurements

The torque measurements were carried out using a Haake twin-screw extruder (Rheomex 252P), equipped with a circular die diameter of 2 mm, to obtain the torque values of the individual polymers. A rotor speed of 30 rpm was used and a total measuring time of 3 min was used for each polymer. The equilibrium torque values, obtained after 3 min of measuring, are reported in Table 1. These values were used to calculate the composition of the blends where phase inversion was expected by using the model of Avgeropoulos [23].

4. Results and discussion

4.1. Co-continuity and phase inversion

The morphologies observed in the 80/20, 60/40, 50/50 and 40/60 PC/PS blend samples from the melt blending, from the re-melt blending in a twin-screw extruder and

Table 1
Torque values of the raw materials

	T (°C)	Torque (N m)
PC	240	135
	260	97
	280	68
PS	240	42
	260	31
	280	20

from the tri-melt blending in an injection-moulding machine are presented in Figs. 1–4, respectively. The micrographs show the PC phase, which remains after the PS phase has been removed. In Figs. 1a–c and 2a–c, we observe that the blends at the compositions of 80/20 and 60/40 PC/PS already formed a well-established dispersed morphology, in which PS forms droplets (dark holes) dispersed in the PC matrix. There are many small irregularly shaped pieces (Figs. 1b and 2a,b), which appear to have originated from the breaking of the PC particles. There are also many highly elongated PC particles as well as many nearly spherical particles (Figs. 1a,c and 2c). In Figs. 3a,b and 4, we observe a co-continuous morphology in the 50/50 and 40/60 PC/PS blend compositions. It is of interest to note from Fig. 4 that the material has been stretched out into many long bamboo-like or rod-like structures. During the sample extracting, we found that the tri-melt blending sample of 50/50 PC/PS blend in the injection-moulding machine and the re-melt blending sample of 40/60 PC/PS blend in the twin-screw extruder had collapsed and become spongy. This indicates that the region of phase inversion of the PC/PS blend might be at a 50/50 PC/PS composition between the second and the third melt blending and at a 40/60 PC/PS composition between the first and the second melt blending. Based on this, we conclude that the blend composition and the blending method determine the formation of co-continuous structures and the point of phase inversion of PC/PS blends. A dispersed morphology is formed when the blend composition is highly asymmetric and a co-continuous morphology is formed when the blend composition is symmetric or close to symmetric.

For the melt blending of PC/PS blends prepared at the heating zones of 240°C, the torque ratio was found to be 3.2, indicating a theoretical point of phase inversion at a 76/24 PC/PS composition calculated from Eq. (2). Increasing the temperature to 260 and 280°C resulted in torque ratios of 3.1 and 3.4, leading to a theoretical point of phase inversion at the 76/24 and 77/23 PC/PS compositions, respectively (see Table 2). However, the blends containing 60–80 wt% PC showed a droplet-matrix morphology (Figs. 1 and 2). The phase inversion was obtained for blends with a PC content of 40 and 50 wt%. These experimental results might be supported by those of Naffa and Henk [11], who observed co-continuous structures at 55 and 60 wt% PC for a blend of PC/PS, prepared in a mixing chamber at 240°C. They found that predicting the theoretical point of phase inversion using Eq. (2) was valid for most of the blends studied, whereas the model also failed for the PC/PS blends. It seems clear from these experiments that the torque ratio is not the only parameter controlling the region for dual-phase continuity in PC/PS blend systems. Our results show that the failure of the model prediction for the PC/PS blend might be explained by the fact that the torque ratio of PC/PS blends is much higher than for the blends investigated by Avgeropoulos et al. [23] and also far away from unity. The location of the region of

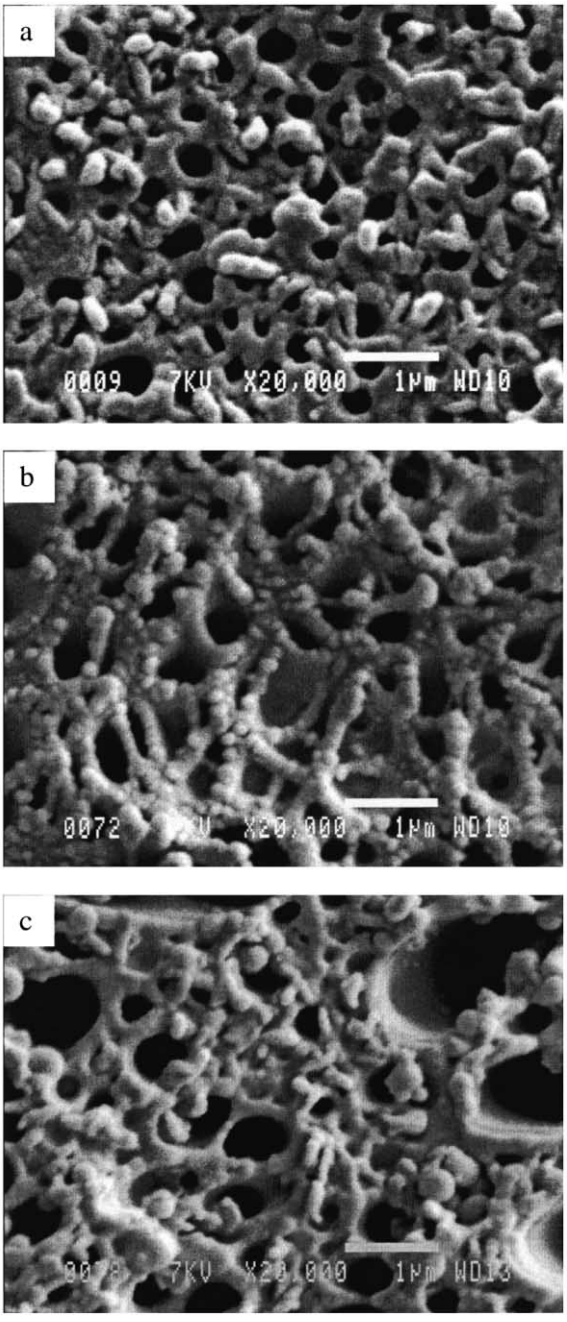

Fig. 1. SEM micrographs after the removal of the PS phase from 80/20 PC/PS blend: (a) first-melt extrusion blend; (b) second-melt extrusion blend; (c) third-melt injection blend.

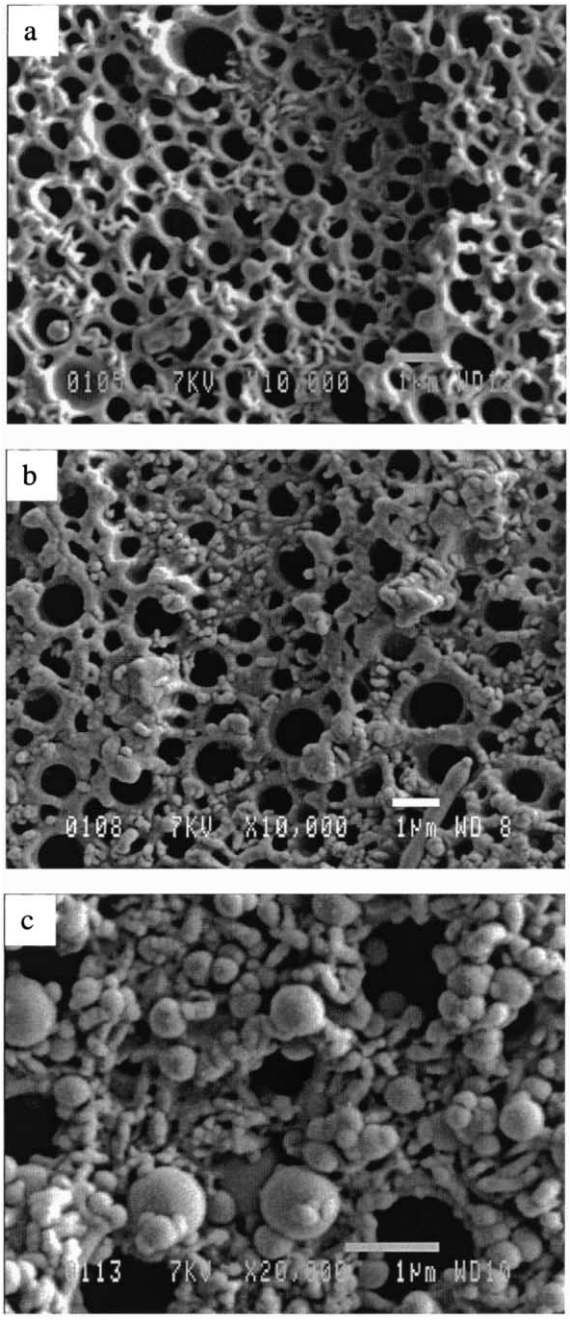

Fig. 2. SEM micrographs after removal of the PS phase from 60/40 PC/PS blend: (a) first-melt extrusion blend; (b) second-melt extrusion blend; (c) third-melt injection blend.

phase inversion is difficult to determine precisely on an industrial scale, but appears to occur between 40 and 50% PC by weight.

4.2. Blade or stratified structure

Figs. 5 and 6 show the SEM images of the PC/PS blends prepared from the quenched samples of each blending method. The morphology observed in the 80/20 PC/PS blends is presented in Fig. 5a–c, where the matrices

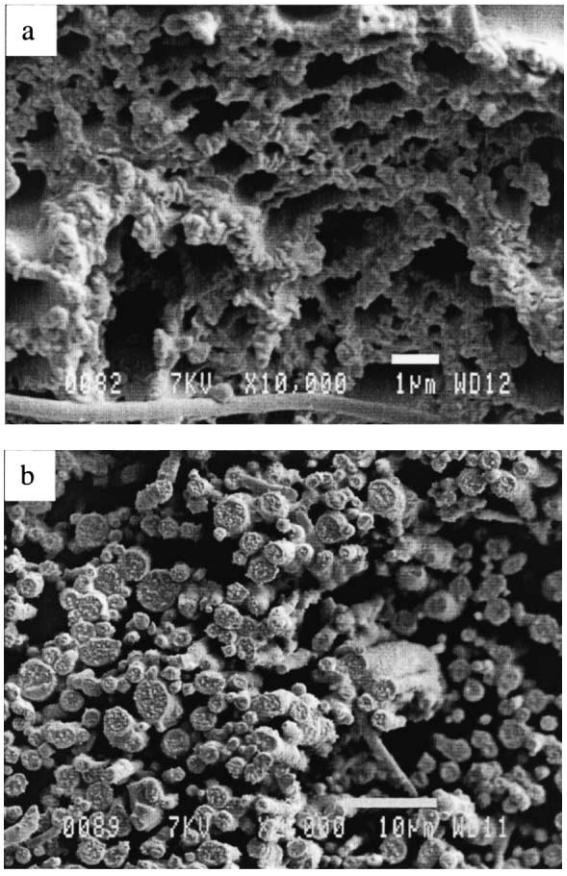

Fig. 3. SEM micrographs after removal of the PS phase from 50/50 PC/PS blend: (a) first-melt extrusion blend; (b) second-melt extrusion blend.

represent the PC phase and the spherical shapes in the matrix represent the PS phase. In Fig. 5a, we observe that the PC phase formed a blade or stratified structure after the first melt blending in the twin-screw extruder, but the blade structure of PC tended to break down (Fig. 5b) after the second melt blending. There are many irregularly small blade or piece shapes (Fig. 5c), which appear to have originated from disintegration of the big blade structure

Fig. 4. SEM micrographs after removal of the PS phase from 40/60 PC/PS blend of the first-melt extrusion.

Table 2
Torque ratios and comparison of theoretical point of phase inversion, calculated from model (2), with experimental results for PC/PS blends

Temperature (°C)	Torque ratio	Theoretical	Experimental
240	3.2	76/24	40–50/60–50
260	3.1	76/24	40–50/60–50
280	3.4	77/23	40–50/60–50

shown above. There are also many small PS spherical particles of diameters from 1 to 2.5 μm dispersed in the PC matrix in Fig. 5a and b. Note that the diameters of the PS spheres in Fig. 5c are in the range of 0.2–1 μm. This might indicate that the blending in the injection-moulding machine could break-up the PS into small particles. Fig. 6a–c shows the morphologies of the 50/50 PC/PS blends. As can be seen from Fig. 6a and b, the blade morphology was formed, but the blade structure of PC/PS blends also began to break-up (Fig. 6c) after the tri-melt blending in the injection-moulding machine.

The morphology of the PC/PS blends, whether blended in a twin-screw extruder or in an injection-moulding machine, has been shown to be quite complex. How the blade or stratified structure is formed is not clear. Very little information is available in the literature concerning PC/PS blend system blended in twin-screw extruder or in injection-moulding machine. It is possible that the blade or stratified structures could be formed and drawn out in the flow field inside the mixer, but that owing to flow and interfacial forces, the blade or stratified structures are unstable and begin to break apart into irregularly shaped pieces.

4.3. Droplet/fibre transitions

One of the most striking features of this study is the significant modification of morphology with radial position in the first extruded strands. Figs. 7 and 8 illustrate this effect at two concentrations for 20 and 40% PC dispersed in PS after the first extrusion. It is evident at both concentrations that a fibrous morphology for the dispersed phase is present at the periphery of the strands. Fig. 7a–c shows the micrographs of the cryogenically fractured cross-section surfaces of the 20/80 PC/PS blends. For 20% PC at the periphery (Fig. 7a), only PC fibre morphologies are observed whereas fibre/droplet morphologies coexist at the midpoint (Fig. 7b) of the sample. Mostly, droplets are observed at the centre (Fig. 7c) of the strand. Fig. 8a–c shows the micrographs of 40% PC phases, which remains after the PS matrix has been removed. From Fig. 8a–c, it can be observed that the presence of fibre or rod-like structures at the periphery (Fig. 8a) is increased significantly and fibre/droplet morphologies also coexist at the midpoint (Fig. 8b), but only droplet morphologies are observed at the centre (Fig. 8c) of the samples. In all the re-melt extrusion samples of the PC/PS blends, only the concentration of 20% PC showed some extended structures (Fig. 9). The PC/PS blend experiments reproducibly show that fibrous morphologies are only found at a specific window of compositions and under specific processing conditions. The composition window for fibre formation is 20–40% PC. In this window, the fibrous morphology is only observed at points in the blend subjected to high shear rates and never in injection-moulded specimens. These results illustrate the importance of the combined effects of both shear rate and composition on the shape of the minor phase. Shear rate effects are greatest at the wall and least at the centre of the strand.

In the literature, two main mechanisms are postulated for extended morphologies. Van-Oene [24] has shown that, in

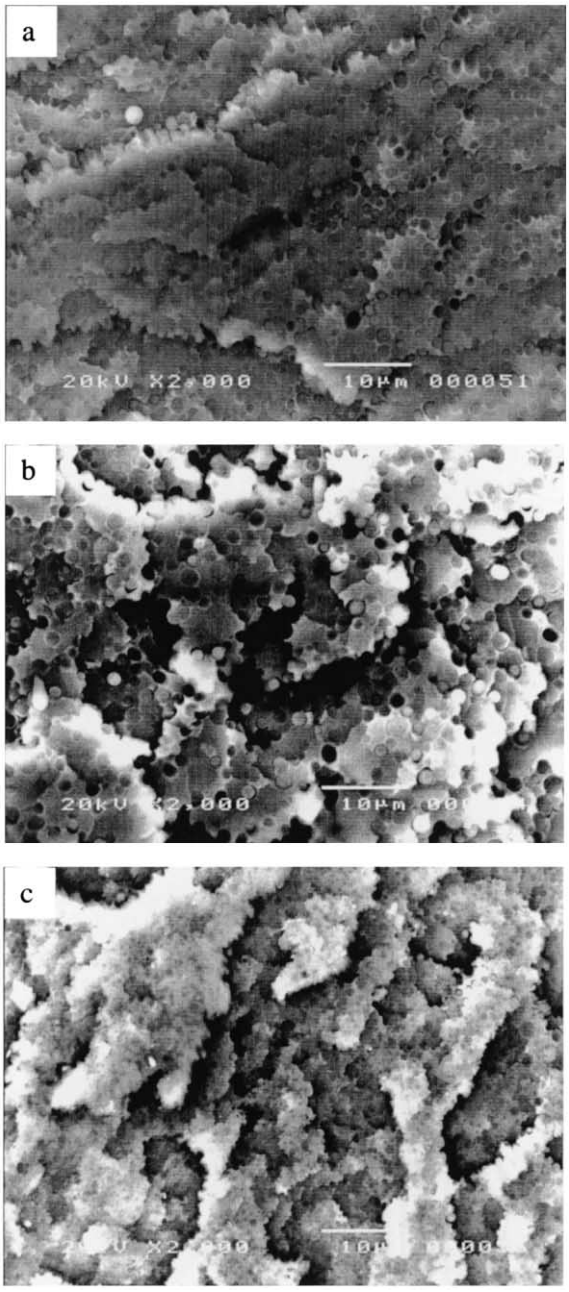

Fig. 5. SEM micrographs for 80/20 PC/PS blend obtained from the cryogenically fractured cross-section surfaces: (a) first-melt extrusion blend; (b) second-melt extrusion blend; (c) third-melt injection blend.

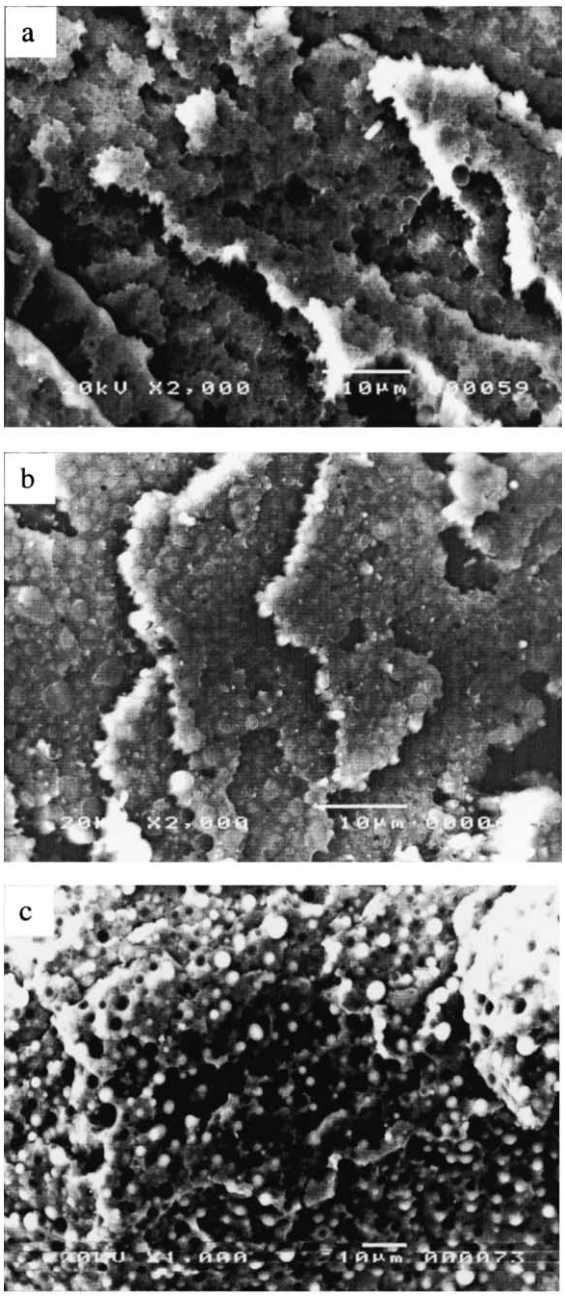

Fig. 6. SEM micrographs for 50/50 PC/PS blend obtained from the cryogenically fractured cross-section surfaces: (a) first-melt extrusion blend; (b) second-melt extrusion blend; (c) third-melt injection blend.

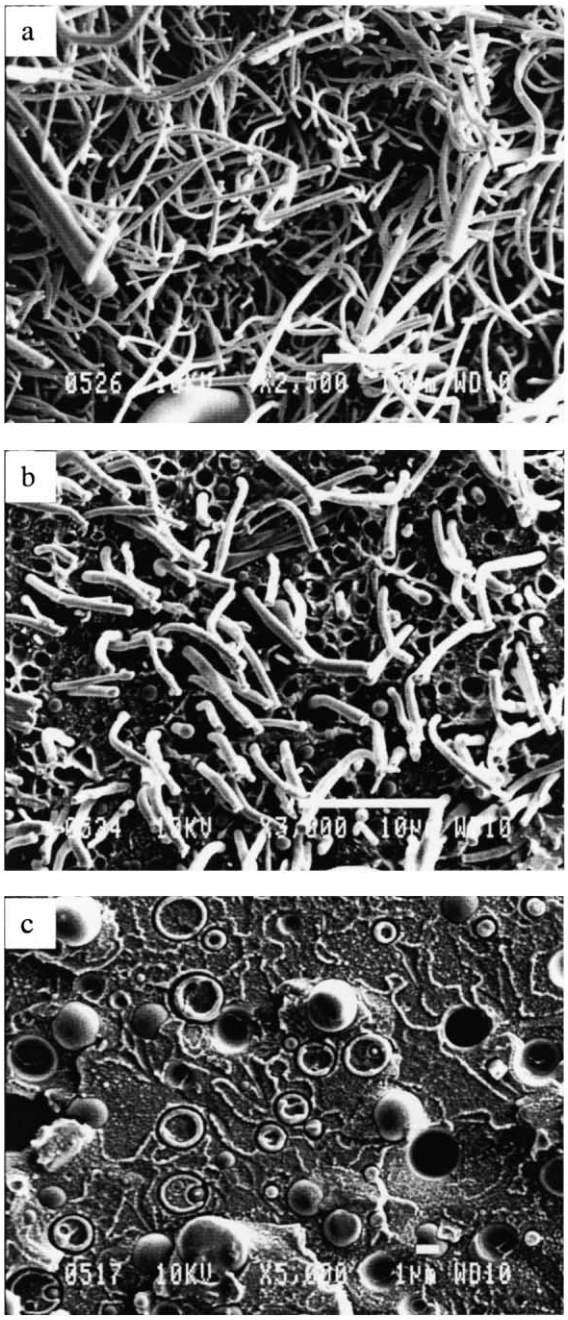

Fig. 7. SEM micrographs for 80/20 PC/PS blend obtained from the cryogenically fractured cross-section surfaces of the first-melt extrusion at three different radial positions: (a) at the periphery; (b) at the midpoint; (c) at the centre.

capillary flow, there are two main modes of dispersion: stratification or droplet formation. These morphologies were shown to be controlled by the particle size, interfacial tension and the differences in the viscoelastic properties of the two phases. Tsebrenko et al. [25] suggested that the main factor governing structure formation processes was the ratio of the melt viscosities, which was varied within very wide limits. These authors found that fibre formation was most pronounced at a melt viscosity ratio close to unity. The above explanations might fit the experimental observation of stratified structures or fibre formation in the PC/PS blends.

5. Conclusions

1. The dual-phase continuity of PC/PS blends is strongly affected by composition and blending method and usually obtained at the point of phase inversion, which can be predicted by a semi-empirical model. In this work, the theoretical prediction of the model for phase inversion deviates from the experimental values.

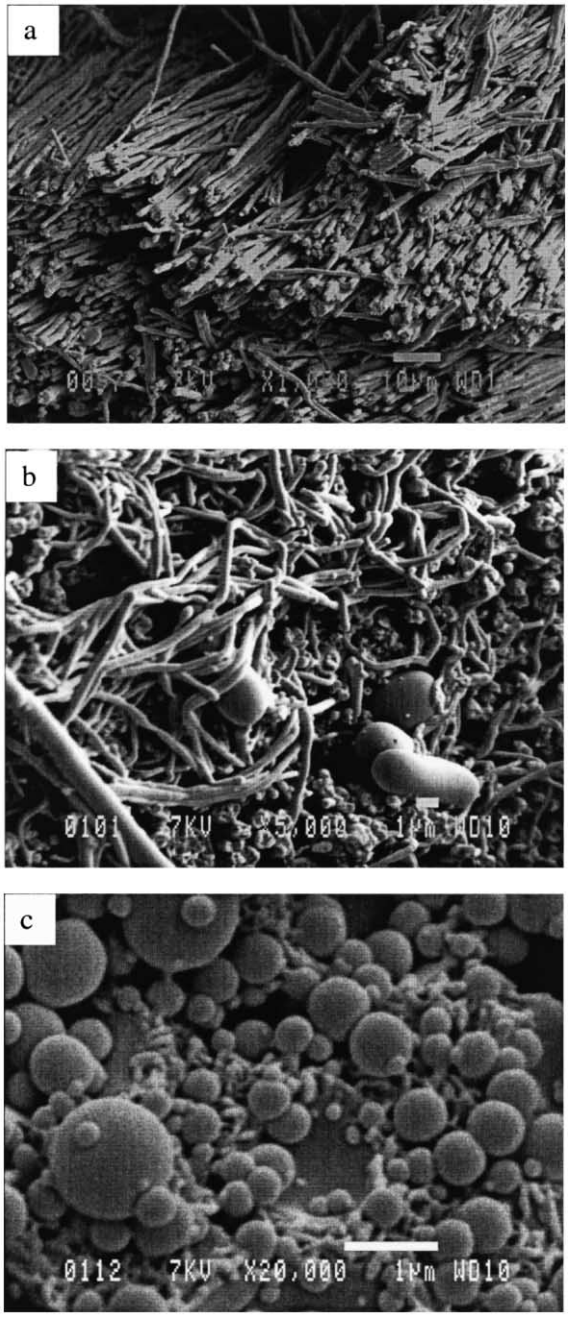

Fig. 8. SEM micrographs after removal of the PS phase from 40/60 PC/PS blend of the first-melt extrusion at three different radial positions: (a) at the periphery; (b) at the midpoint; (c) at the centre.

2. Some blade or stratified structures are formed and drawn out in the flow field inside the PC/PS blend mixer. Owing to interfacial and flow forces, these blade or stratified structures may be broken down into small blade or stratified pieces in some compositions of PC/PS blends.
3. The results obtained clearly demonstrate that the presence of fibre or rod-like structures is favoured by higher shear rate (proximity to the die wall).

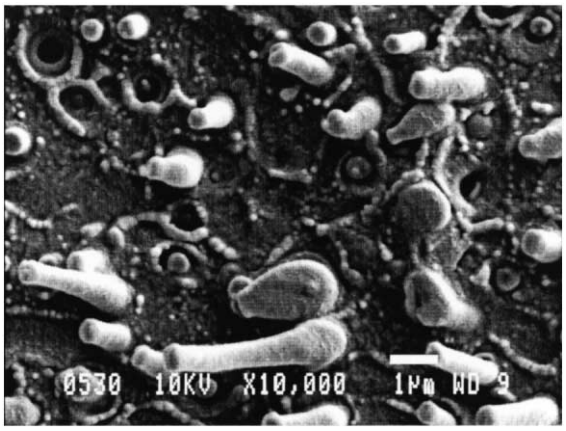

Fig. 9. SEM micrographs for 20/80 PC/PS blend obtained from the cryogenically fractured cross-section surfaces of the re-melt extrusion.

Acknowledgements

The financial support of the Technical Science Council of Denmark is gratefully acknowledged. The authors would like to thank Mr Palle V. Jensen for his help with the SEM work, Professor David Plackett for his help with the discussion of this manuscript.

References

[1] Utracki LA. Polymer alloys and blends. New York: Hanser, 1989.
[2] Wu S. Polymer 1985;26:1855.
[3] Hobbs S. Polym Engng Sci 1986;26:74.
[4] Borggreve RJM, Gaymans RJ, Schuijer J, Housz JFI. Polymer 1987;28:1489.
[5] Stell JR, Paul DR, Barlow JW. Polym Engng Sci 1976;16:496.
[6] Van Gheluwe P, Favis BD, Chalioux JP. J Mater Sci 1988;23:3910.
[7] Kamal MR, Jinnah IA, Utracki LA. Polym Engng Sci 1984;24:337.
[8] Jiasong H, Wensheng B, Jijun Z. Polymer 1997;38:6347.
[9] Lyngaae-Jørgensen J, Lunde Rasmussen K, Chtcherbakova EA, Utracki LA. Polym Engng Sci 1999;39:1060.
[10] Favis BD, Therrien D. Polymer 1991;32:1474.
[11] Nafaa M, Henk V. Polymer 1996;37:4069.
[12] Favis BD. J Appl Polym Sci 1990;39:285.
[13] Tsebrenko MV. Int J Polym Mater 1983;10:83.
[14] Min K, White JL, Fellers JF. Polym Engng Sci 1984;24:1327.
[15] Jordhamo GM, Manson JA, Sperling LH. Polym Engng Sci 1986;26:517.
[16] Utracki LA. J Rheol 1991;35:1615.
[17] Cartier H, Hu GH. Polym Engng Sci 1999;39:996.
[18] Rolando RJ, Chan HT. Polym Engng Sci 1992;32:1814.
[19] Chris ES, Christopher WM. Polymer 1994;35:5422.
[20] Lee JK, Han CD. Polymer 1999;40:6277.
[21] Amash A, Zugenmaier P. Polymer 2000;41:1589.
[22] Paul DR, Barlow J. J Macromol Sci, Rev Macromol Chem C 1980;8:9.
[23] Avgeropoulos GN, Manson JA, Sperling LH. Polym Engng Sci 1986;26:517.
[24] Van-Oene H. J Colloid Interf Sci 1972;40:448.
[25] Tsebrenko MV, Yudin AV, Ablazova TI, Vinogradov GV. Polymer 1980;17:831.